Separation Science and Technology
Publication details, including instructions for authors and subscription information:
http://www.informaworld.com/smpp/title~content=t713708471

Regeneration of a Fixed Bed of Activated Carbon Adsorbed Organic Vapor by Using Hot Nitrogen Purge

Chen-Chia Huang[a]; Tzyy-Ling Hwu[a]; Yen-Sheng Hsia[a]
[a] DEPARTMENT OF APPLIED CHEMISTRY, CHUNG CHENG INSTITUTE OF TECHNOLOGY, TAIWAN, REPUBLIC OF CHINA

To cite this Article Huang, Chen-Chia , Hwu, Tzyy-Ling and Hsia, Yen-Sheng(1993) 'Regeneration of a Fixed Bed of Activated Carbon Adsorbed Organic Vapor by Using Hot Nitrogen Purge', Separation Science and Technology, 28: 15, 2431 — 2447
To link to this Article: DOI: 10.1080/01496399308019747
URL: http://dx.doi.org/10.1080/01496399308019747

SEPARATION SCIENCE AND TECHNOLOGY, **28**(15&16), pp. 2431–2447, 1993

Regeneration of a Fixed Bed of Activated Carbon Adsorbed Organic Vapor by Using Hot Nitrogen Purge

CHEN-CHIA HUANG,* TZYY-LING HWU, and
YEN-SHENG HSIA
DEPARTMENT OF APPLIED CHEMISTRY
CHUNG CHENG INSTITUTE OF TECHNOLOGY
TASHI, TAOYUAN, 335, TAIWAN, REPUBLIC OF CHINA

ABSTRACT

Thermal regeneration of activated carbon adsorbed acetone or acetaldehyde was studied experimentally and theoretically by hot nitrogen purging through a fixed bed. A linear driving force mass transfer model was proposed and found to well simulate the experimental data. The parameters investigated included total system pressure, initial bed loading, and regeneration temperature. The temperature of purge gas was programmed by some different modes. The adsorption isotherms were determined by a static manometric method.

INTRODUCTION

Activated carbons for recovery of volatile organic compounds (VOCs) from fluid streams have been used in industry for many years (1–4). After saturation, the VOC-laden spent activated carbon is either replaced with fresh adsorbent or regenerated on site. Since it is an important step, dominant in the economic success of the environmental treatment processes, a number of methods to regenerate spent activated carbons have been proposed (3–6). The alternatives available include thermal regeneration by steam or hot gas, using heating coils inside the bed, and vacuum regeneration. Recently, Petkovska et al. (7) proposed a "electrothermal desorption" by passing an electric current through adsorbent particles. When

* To whom correspondence should be addressed.

the adsorbates include high molecular weight or strongly adsorbable compounds, thermal regeneration at high temperature is generally used. As the adsorbates are smaller molecules, a lower temperature thermal regeneration is possible to employ.

Klobucar and Pilat (8) investigated the design and operating parameters of a continuous flow countercurrent thermal desorber to purge ethanol out by a hot air stream. For a fixed-bed adsorber, the standard process consists of the following three-step cycles: (a) adsorption, (b) desorption, and (c) cooling. Basmadjian (9) proposed some criteria for the omission of the cooling step. Steaming is the most widely used method for regeneration of activated carbon beds. The solvent-steam effluent mixture is condensed and sent to appropriate separation devices. When the solvent forms an azeotrope with water, the mixture separation can become more difficult. This rapidly increases further capital and operating expenses for the process. In contrast, if a desorption process employs an inert gas as a regenerant, the solvent is easily recovered in a condenser. Basmadjian et al. (10) and Kumar and Dissinger (11) considered the nonisothermal removal of adsorbed carbon dioxide from a fixed bed of 5A zeolite using a hot nitrogen purge. Schork and Fair (12) studied desorption of propane from carbon by using a hot nitrogen purge through a fixed bed. In those studies, a characteristic temperature was found for which energy consumption is a minimum. Davis and LeVan (13) investigated thermal swing adsorption (TSA) cycles with and without a cooling step and tried to find the optimal performance of an adsorber. Yet most of previous work on TSA processes employed a constant regeneration temperature for the desorption step. Kulvaranon et al. (14) investigated a desorption process with multisteps increasing temperature and resulting in an effective separation of two adsorbed components.

The purposes of this paper include developing a mathematical model for simulating a thermal regeneration process for spent carbon in a fixed bed and collecting the pertinent experimental data. The present paper focuses upon such operating parameters as pressure and temperature. A stepwise thermal regeneration process is investigated to possibly provide a constant effluent concentration from a fluctuant feed source at the adsorption step.

THEORETICAL MODEL

For developing a dynamic model of a fixed-bed adsorber, the following assumptions were made. The system pressure, carrier gas flow rate, and feed concentration were assumed to be held constant. The gas phase was assumed to obey the ideal gas law. Radial temperature, concentration,

and velocity gradient within the bed were neglected. Accumulation of carrier gas in the pores of the adsorbent was disregarded. The heat capacity of the gas within pores of the solid phase was negligible comparing to that of the solid. Axial conduction within the column wall was ignored. But both axial dispersions of mass and energy were considered. The intraparticle heat-transfer resistance was negligible. The gas phase was dilute in this study, and the physical properties of the gas phase were assumed to be those of the carrier gas and calculated as a function of temperature. The physical properties of the adsorbent and column wall were assumed to be constant. Material and energy balances could be easily set up based on the assumptions mentioned above.

The initial gas- and solid-phase concentrations for the adsorption step are zero. For the regeneration step, they are the values of final conditions of the previous adsorption step. The concentration and temperature of influent stream at inlet boundary are maintained constant. For the regeneration step, however, the temperature of the purge gas is programmed and is a function of time.

A linear driving forced model was employed to calculate the overall mass transfer rate. Generally, there are three mass transfer steps in an adsorption process: fluid–film transfer, pore diffusion, and surface diffusion. An effective overall mass transfer coefficient could be derived as follows (12):

$$\frac{1}{K_0} = \frac{1}{k_f} + \frac{R_p}{5D_{eff}} \tag{1}$$

where D_{eff} is an effective pore diffusivity which includes Knudsen pore diffusivity and surface diffusivity.

$$D_{eff} = D_K + \frac{D_s \rho_s}{C} \frac{\partial w}{\partial y} \tag{2}$$

The surface diffusion is an activated process which can be expressed by an Arrhenius-type expression (15)

$$D_s = D_{so} \exp(-0.45\Delta H/RT) \tag{3}$$

The Petrovic and Thodos correlation (16) could be employed for the film transfer coefficient for the low Reynolds number region covered in the present study.

$$k_f = \frac{0.357}{\epsilon} \mathrm{Re}^{0.64} \mathrm{Sc}^{0.33} \frac{D_m}{2R_p} \tag{4}$$

The effective axial dispersion coefficient and thermal conductivity could be estimated by models reviewed by Ruthven (17).

This model was employed to simulate both adsorption and desorption processes. The numerical method of lines was chosen for solving the model of partial differential equations. The spatial dimensional was discretized into 24 grid points by using a second-order central differencing. The resulting set of ordinary differential equations was then solved by using the LSODE solver (18).

EXPERIMENTAL

A granular pellet type of BPL 4 × 6 activated carbon, manufactured by the Calgon Corporation, was employed as an adsorbent. The physical properties of carbon provided by the manufacturer are listed in Table 1. The adsorbates were acetone vapor and acetaldehyde vapor. The acetone and acetaldehyde employed were an instrument grade (99.5%) supplied by Nihon Shiyaku Industries and Riedel-de Haën, respectively.

The equilibrium isotherms of organic solvent vapors onto activated carbon were determined manometrically. A vacuum pump and a diffusion pump in combination provided a manifold vacuum down to 0.01 Pa. The system pressure was monitored by a pressure transducer and a four-digit display indicator. Whenever the pressure reading held for more than 20 minutes, it was assumed an equilibrium state had been reached. During data acquisition, sample bottles were maintained isothermally by a water bath with an immersion circulator to ensure temperature uniformity.

A bench-scale unit was used to study dynamic adsorption and hot purge regeneration processes. A schematic flow diagram of the equipment is shown in Fig. 1. Nitrogen of 99.9% purity was used as the carrier gas during the adsorption phase and as the regenerant during the desorption phase. The flow rate of nitrogen was measured and digitally displayed by a Hastings-Teledyne mass flowmeter. The saturated vapor of acetone or acetaldehyde was bubbled and carried by a branch stream of nitrogen through two saturators in series in a thermostat. This stream was then mixed with the pure nitrogen stream. The fixed-bed adsorber was fabricated from a 4.27-cm o.d. stainless steel tubing with a 0.135-cm thick wall.

TABLE 1
Physical Properties of BPL 4 × 6 Activated Carbon

Total surface (BET method), m^2/kg	1.05×10^6–1.15×10^6
Pellet diameter, m	3.4×10^{-3}–4.0×10^{-3}
Apparent density, kg/m^3	480–510
Voids in packed bed	0.43

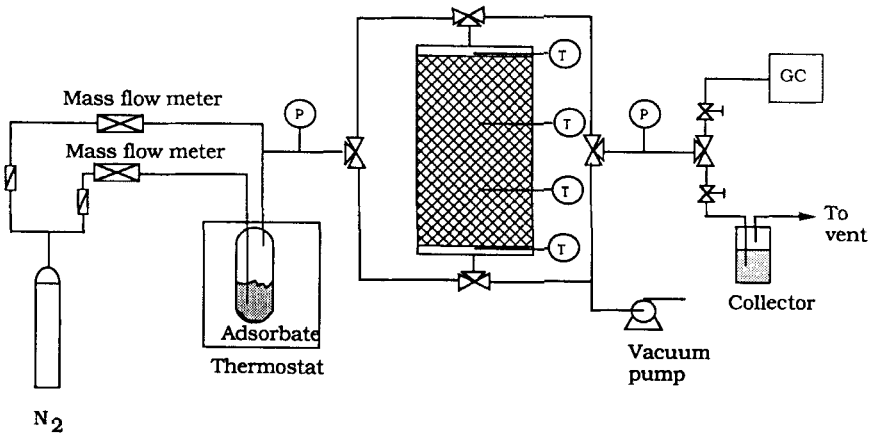

FIG. 1 Schematic diagram of dynamic experimental apparatus.

The column was 30 cm long and packed to a height of 26.3 cm with carbons. Two fine mesh stainless steel screens were placed at the top and bottom of the bed to hold up the carbon and to prevent fluidization of the packing during pressure transients. Before packing, the carbon was boiled in water and then dried in a vacuum oven. The column was wrapped with heating tape and insulated with a 5-cm thick layer of fiberglass. To achieve uniform distribution and to avoid possible end effects, Pyrex glass beads (0.3 cm in diameter) were packed at both the top and bottom of the column. Two thermocouples were installed above and below the top and the bottom of the screens, about 0.2 cm away, to monitor the temperatures of the influent and effluent. The other two thermocouples were inserted along the axial centerline of the bed at one-third the distance of the carbon section from both ends. Two surface thermocouples were attached onto the outside of the bed at the corresponding points. The effluent was continuously detected by a HP 5890A gas chromatograph with a flame ionization detector and a HP 3390A integrator data-acquisition system. Adsorber pressure was controlled by a back-pressure regulator. Before performing the adsorption operation, the column was vacuumed and heated to 473 K overnight, then cooled to room temperature. After the adsorption experiment, the carbon bed was regenerated by hot nitrogen flowing in the opposite direction to purge the adsorbate from the adsorbent. The purge gas temperature was controlled by an Eurotherm type 818P PID Controller. The propagation of a thermal wave through the bed was monitored with thermocouples connected to an Eurotherm Type 141 digital indicator.

RESULTS AND DISCUSSION

Equilibrium Isotherm

Typical isotherm data of acetone and acetaldehyde on BPL 4 × 6 activated carbons are presented in Fig. 2. The amount of acetaldehyde vapor adsorbed on BPL carbon at 19.2 kPa and 293 K was found to be 0.517 g per g of carbon. An adsorption capacity of 0.473 g acetone per g of carbon was found at 20.9 kPa and 293 K. The experimental isotherm data are consistent with literature data (1, 19, 20). From Fig. 2 it can be seen that at a lower partial pressure, acetone is more adsorbed on BPL carbon than is acetaldehyde. However, at higher pressure the amount of acetaldehyde vapor adsorbed on BPL carbon is greater than acetone.

A temperature-dependent form of the Langmuir-Freundlich isotherm equation (21) was found to provide a good correlation of equilibrium data.

$$w = \frac{ab(Py)^d e^{c/RT}}{1 + b(Py)^d e^{c/RT}} \tag{5}$$

There are four adjustable parameters in Eq. (5). The appropriate sets of constants determined by an unconstrained nonlinear programming package are listed in Table 2. The average relative deviations of acetone–carbon and acetaldehyde–carbon systems are less than 1.5 and 4.3%, respectively. The correlation results are plotted along with the experimental data in Fig. 2.

Dynamic Runs

Ten adsorption and desorption dynamic cyclic runs were made. Operating conditions are listed in Table 3. An adsorption step and the subsequent regeneration step included in a cyclic process were represented by the same run number. The adsorbate concentrations of the inlet gas stream for adsorption runs ranged from 3.4 to 5.0 mol%. The system pressure was maintained constant in a range between 136 and 170 kPa. The temperature of the inlet gas for adsorption runs was about room temperature. The

TABLE 2
Best Fit Parameters of Langmuir–Freundlich Isotherm Equation

Adsorbate	a (mol/g carbon)	b $(\text{kPa})^{-d}$	c (J/mol)	d
Acetone	8.7×10^{-3}	1.197×10^{-4}	2.29×10^{4}	0.699
Acetaldehyde	1.5×10^{-2}	2.354×10^{-5}	2.24×10^{4}	0.832

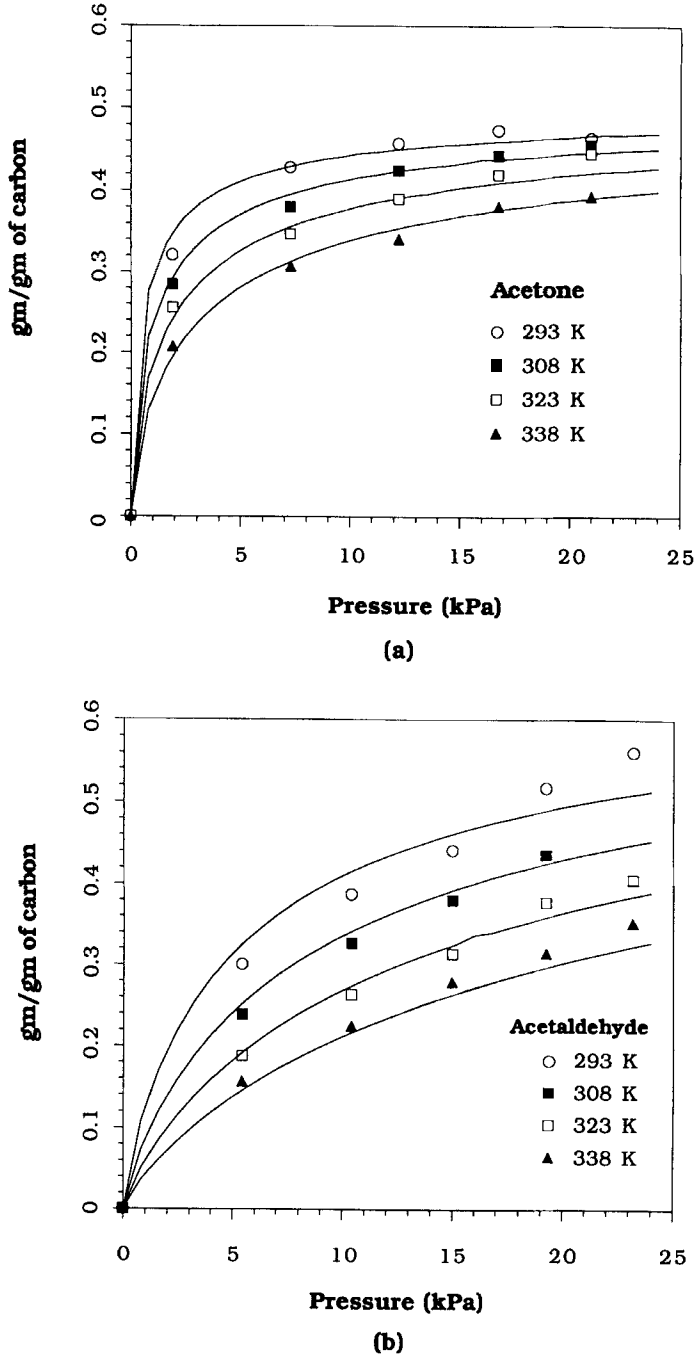

FIG. 2 Adsorption isotherms of acetone (a) and acetaldehyde (b) on BPL activated carbon.

TABLE 3
Operating Conditions of Adsorption Desorption Runs[a]

		Adsorption				Regeneration		
Run	Adsorbate	Y_{in} (%)	$G \times 10^3$ (kmol/m^2·s)	T_{in} (K)	P (kPa)	$G \times 10^3$ (kmol/m^2·s)	T_{reg} (K)[b]	P (kPa)
17	Acetone	3.4	3.50	297	170	3.38	#1	170
25	Acetone	5.0	3.52	297	136	3.34	478	136
26	Acetone	4.7	3.55	297	170	3.38	478	170
33[c]	Acetone	4.5	3.54	298	136	3.38	478	136
34	Acetone	5.0	3.52	299	136	3.34	#2	136
65	Acetaldehyde	4.6	3.76	300	136	3.58	478	136
66	Acetaldehyde	4.9	3.76	300	170	3.58	478	170
73[c]	Acetaldehyde	4.7	3.76	299	136	3.58	478	136
74	Acetaldehyde	4.9	3.76	299	136	3.58	#2	136
75	Acetaldehyde	3.8	3.73	299	136	3.58	#3	136

[a] Adsorption steps carry the prefix AD-, and the corresponding regeneration steps carry the prefix DE-.

[b] #1: A programmed stepwise regeneration temperature started from 303 K to 323, 353, 393, 433, and 483 K at a heating rate of 5 K/min, and holding for 30, 60, 45, 30, and 49 minutes at each plateau temperature, respectively. #2: A programmed regeneration temperature started at 303 K with a heating rate of 4 K/min until 478 K, then held until regeneration is complete. #3: Operating condition the same as that of #2, but with a heating rate of 8 K/min.

[c] For partial saturation the adsorption run was terminated at the first detection of adsorbate.

regeneration temperatures of most of runs were 478 K. The regeneration temperatures of Run DE-17, 34, 74, and 75 were started at 303 K with different heating programs. The adsorption experiments were stopped when the effluent concentration approached 95% of the feed concentration, and the desorption steps were terminated when the effluent concentration was around 1% of the corresponding adsoption feed concentration.

According to the energy balance equations, the values of the heat transfer coefficients, U and h_w, were evaluated by simulating pure nitrogen heating data. The best fit values of U and h_w were 2.38 and 19.8 J/m^2·s·K, respectively. All these values were retained for use in the adsorption and regeneration simulations.

To estimate surface diffusivity D_s, Eq. (3) was employed. The preexponential factor D_{so} is the only adjustable parameter for determining the overall mass transfer coefficient. The remaining diffusivities and transfer coefficients were estimated by the appropriate correlations as mentioned above. In this study the best fit values of D_{so} for acetone and acetaldehyde

onto activated carbon are 7.74×10^{-8} and 6.97×10^{-8} m^2/s, respectively. These values of D_{so} were used for all simulation runs. Figure 3 shows a typical comparison of experimental data and corresponding modeling results for the dynamic adsorption of acetaldehyde vapor onto and desorption from a BPL carbon bed. In this paper a linear driving force model was used to account for the lumped effects of mass transfer resistances. As can be seen, the model fits the experimental data very well. During the first few minutes of the regeneration step (the dip region of the depletion curve), the predicted exit concentration is lower than the experimental data. This deviation can be attributed to heat loss from the bed during the interval between adsorption and desorption, which influenced the initial condition of the regeneration but was not accounted for in the model.

Several different temperature-programmed thermal regeneration processes were employed for desorption. Figure 4 illustrates the depletion curve of a five-step temperatures desorption process (DE-17). The system operating conditions were held substantially constant, but the temperature increased gradually at a constant rate of 5 K/min. As shown in Fig. 4, the effluent concentration of acetone held almost constant. This implies that it is possible to recover a stable solvent concentration from gas streams.

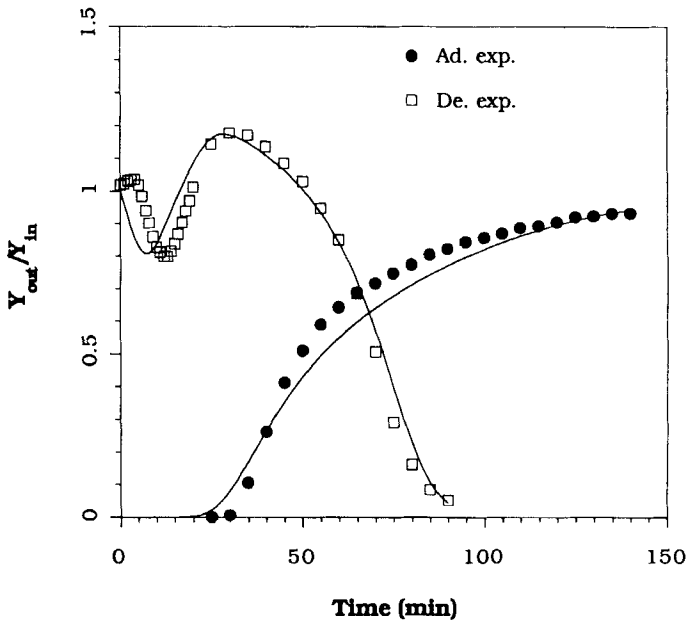

FIG. 3 Simulation of experimental Run 65. See Table 3 for operating conditions.

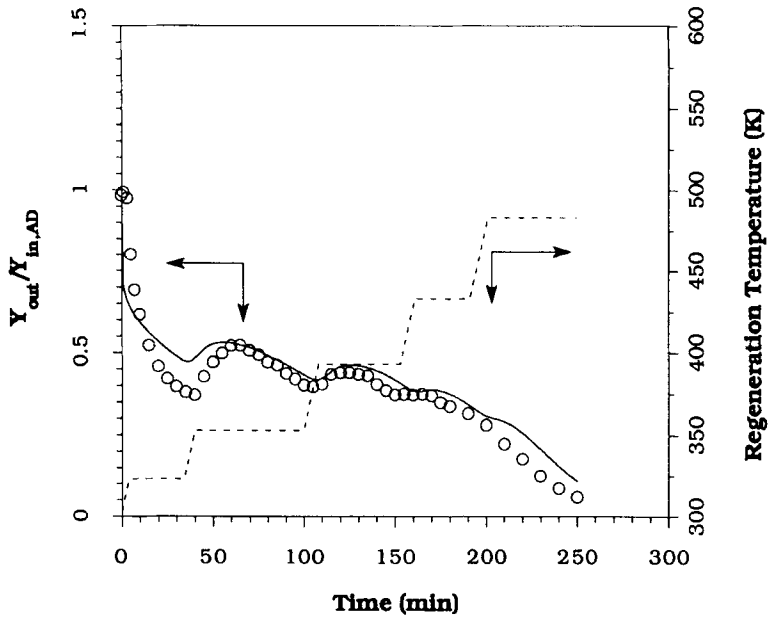

FIG. 4 Data and simulation for experimental Run DE-17 (stepwise thermal regeneration). See Table 3 for operating conditions.

Figure 5 compares the depletion curves using a temperature-programmed regeneration at different heating rates. Both Runs DE-74 and DE-75 were started at 303 K. The former experiment was run at a heating rate of 4 K/min while the latter was heated at a rate of 8 K/min. Run DE-75 shows that purge gas from the higher heating rate experiment caries more energy to desorb molecules from carbon.

Figures 6–9 are based on simulation of an adiabatic adsorber of the same size as was used in the experimental study. The basic operating conditions were the same as those of Runs 25 and 66 for acetone and acetaldehyde runs, respectively. For regeneration runs, the purge gas temperature was set at the characteristic temperatures of acetone and acetaldehyde (439 and 413 K, respectively). Variations from the basic conditions are noted in the following discussion.

The effect of total bed pressure on both breakthrough and depletion curves is presented in Fig. 6. Breakthrough times for both adsorbates are apparently longer at higher bed pressure runs. It is expected that an increase of system pressure may lead to a higher bed loading and result in a longer breakthrough time. The breakthrough curves at higher pressure

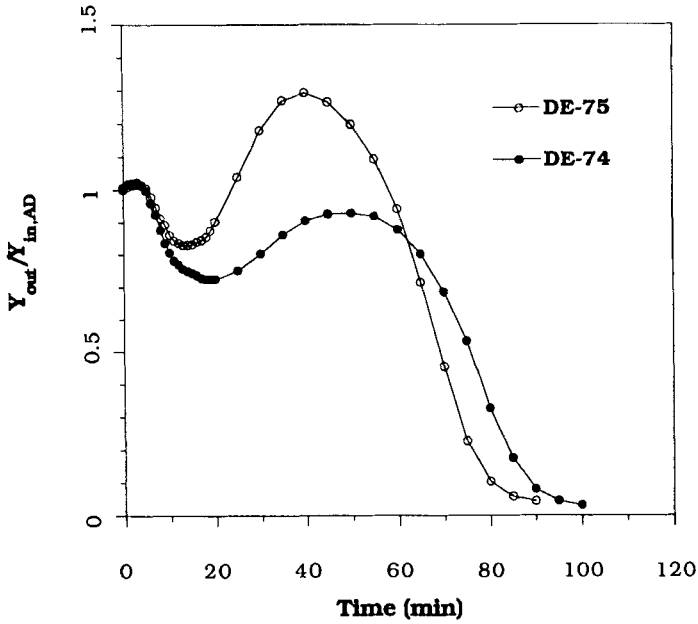

FIG. 5 Comparison of depletion curves by a temperature-programmed regeneration with different heating rates. See Table 3 for operating conditions.

are steeper than those at lower pressure. The breakthrough curves of acetone are sharper than those of acetaldehyde at the same operating pressure. In lower pressure runs, the breakthrough time of acetaldehyde is much shorter than that of acetone. This implies that acetone is more strongly adsorbed than acetaldehyde. This is consistent with the results of static equilibrium isotherm measurements. The partial pressure of the adsorbate is about 25 kPa when the total system pressure is higher than 506.5 kPa. Figure 2 shows that the adsorptions of both vapors are almost the same. Accordingly, the break points in Fig. 6 are quite close for both adsorbates, although the mass transfer zone for acetaldehyde is wider than that for acetone. Regeneration takes longer at higher pressure. In other words, higher pressure is unfavorable for hot purge regeneration. A similar result was reported by Huang and Fair (22).

To confirm the effect of system pressure on regeneration, a study was made based on the same operating conditions as were used for the adsorption steps. Figure 7 illustrates the depletion curves of acetaldehyde at different regeneration pressures. The bed pressure was maintained at 135.8 kPa for adsorption. The system pressure ranged from 101.3 to 303.9

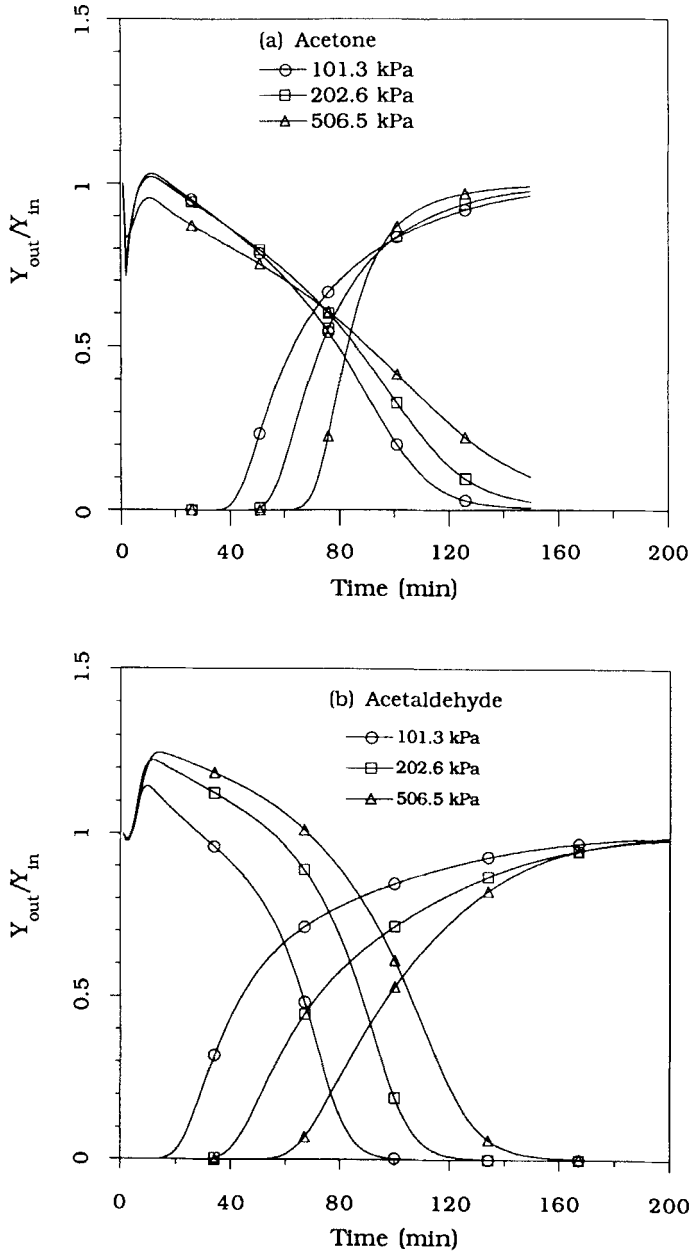

FIG. 6 Effect of pressure on both breakthrough and depletion curves: (a) acetone and (b) acetaldehyde. Based on simulation of an adiabatic adsorber.

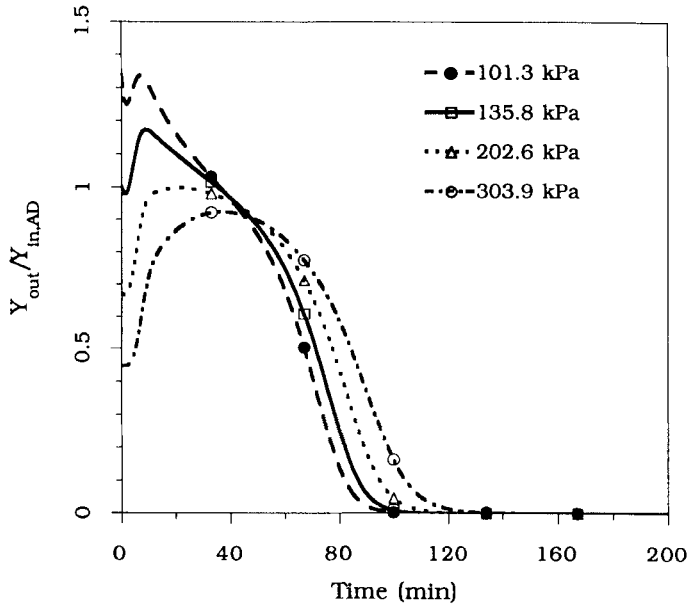

FIG. 7 Effect of pressure on regeneration of carbon that has adsorbed the same amount of acetaldehyde. Based on simulation of an adiabatic adsorber.

kPa for the desorption steps. The mole fraction ratios of adsorbate in the effluent stream to that in the influent stream were adjusted according to pressure changes. It is observed that a higher regeneration pressure results in a higher effluent concentration and a longer regeneration time. As the pressure is reduced, the maximum concentration leaving the bed is reduced. The regeneration time is shorter at lower pressure. A similar result was found by Davis and LeVan (13). Nevertheless, a high-pressure purge gas is more favorable for removing adsorbate from a carbon bed when a concentrated vapor is desired.

The effect of initial bed loading is shown in Fig. 8. The simulation was conducted with a low feed concentration (0.1%) to eliminate the possibility of heat effects. Although the adsorption times were different, the temperature distributions in the adsorber were similar. Bed loading is a function of the operating time at the adsorption step. From Fig. 8 it is observed that the total regeneration times of these four runs were almost identical. The roll-up values of depletion curves were quite different. As expected, the peak height of the depletion curve is higher at a larger initial bed loading. The insensitivity of regeneration time to level loading indicates

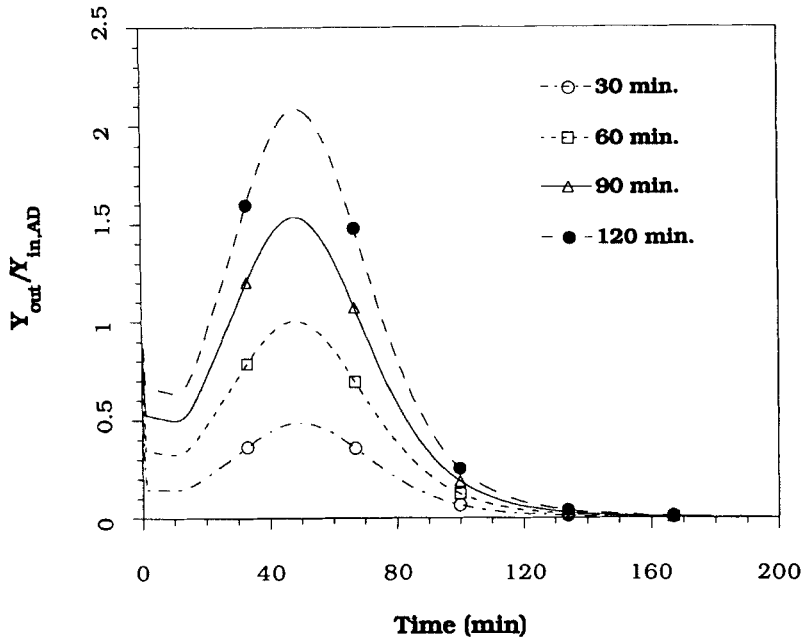

FIG. 8 Effect of initial bed loading on regeneration depletion curves of acetone adsorbate. Based on simulation of an adiabatic adsorber.

that the required desorption time will not be affected by fluctuations in the feed concentration during the adsorption step. A similar result was reported by Basmadjian et al. (10).

Figure 9 shows the simulation results of three regeneration runs for an adiabatic carbon bed adsorbing the same amount of acetaldehyde. Run A was started regenerating by nitrogen purge gas from 311 to 413 K at a heating rate of 2.8 K/min, then held at 413 K until desorption was complete. The total regeneration time of Run A was 116 minutes. Run B was carried out from 413 to 311 K by decreasing the heating rate to 2.8 K/min; the temperature was kept constant. Based on the same energy carried by the purge gas, Run C was designed to start at 413 K for 79 minutes, then decrease at a rate of 2.8 K/min until 311 K was reached. Based on Fig. 9, the regeneration time of Run C was the shortest when the effluent concentration was less than 1% of the corresponding adsorption feed concentration. Although the energy requirement was the lowest, the regeneration time of Run B was too long. Therefore, it is better to regenerate a carbon bed by starting with a high purge gas temperature for an appropri-

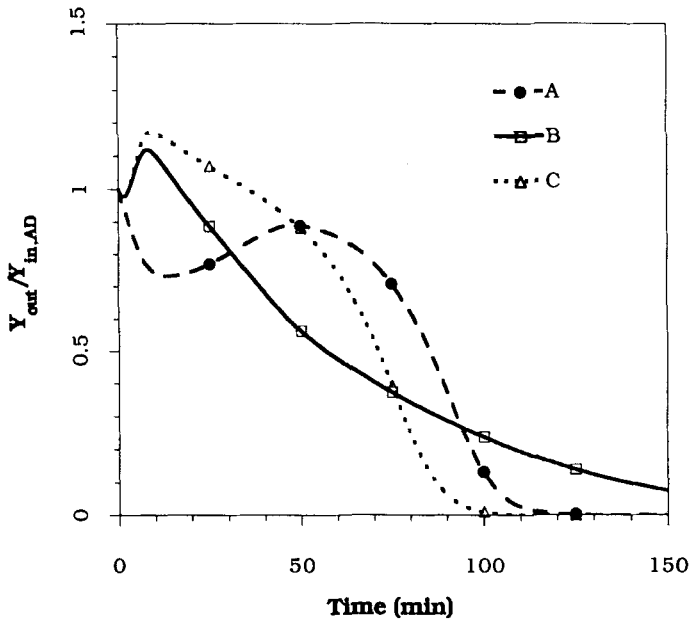

FIG. 9 Acetone depletion curves of different temperature-programmed regeneration processes. Based on simulation of an adiabatic adsorber.

ate time period followed by a decreasing purge gas temperature. On the same energy base, regeneration time and purge gas are saved by purging at a higher temperature.

CONCLUSIONS

BPL activated carbon is suitable for the recovery of acetone and acetaldehyde vapors from gas streams. The adsorption capacity of acetone is larger than that of acetaldehyde at a lower partial pressure. However, at high pressure the adsorption amount of acetaldehyde on BPL carbon is larger than that of acetone.

The proposed linear driving force model simulates the dynamic experimental data of a fixed-bed adsorber very well. For hot purge regeneration, a lower system pressure is economical. Nevertheless, a high-pressure purge gas is more favorable if a concentrated vapor is required. Regeneration time and purge gas requirement are minor functions of the initial bed loading. Desorption time is not affected by fluctuations in the feed concentration during the adsorption phase. A variable-temperature step-

wise desorption process could be designed to obtain a stable concentration of recovery solvents. A temperature-programmed regeneration process starting with a higher temperature would be more efficient for shortening the desorption time and reducing the consumption of purge gas.

NOMENCLATURE

a, b, c, d	constants of isotherm equation
C	gas stream concentration (kmol/m^3)
D_{eff}, D_K, D_m, D_s	effective, Knudsen, molecular, and surface diffusivity, respectively (m^2/s)
D_{so}	preexponential factor in the surface diffusion (m^2/s)
h_w	heat transfer coefficients for column wall (J/cm^2·s·K)
ΔH	heat of adsorption of adsorbate onto carbon (J/mol)
k_f	fluid film mass transfer coefficient (m/s)
K_0	effective overall mass transfer coefficient (m/s)
P	total pressure (kPa)
R	gas constant
Re	Reynolds number
R_p	radius of pellet (m)
Sc	Schmidt number
T	temperature (K)
U	overall heat transfer coefficient for column insulation (J/m^2·s·K)
w	amount of adsorbate adsorbed onto carbon (g/g of carbon)
y	adsorbate mole fraction in gas phase (mol%)

Greek Letters

ϵ	void fraction in a bed
ρ_s	particle density (kg/m^3)

ACKNOWLEDGMENT

This work was financially supported by the National Science Council, Republic of China, under Contract NSC 79-0402-E-014-01.

REFERENCES

1. F. G. Sawyer and D. F. Othmer, *Ind. Eng. Chem.*, *36*(10), 894 (1944).
2. E. S. Larsen and M. J. Pilat, *Environ. Prog.*, *10*(1), 75 (1991).

3. P. C. Wankat and L. R. Partin, *Ind. Eng. Chem., Process Des. Dev., 19*(3), 446 (1980).
4. J. F. Scamehorn, *Ibid., 18*(2), 210 (1979).
5. P. Harriott and A. T.-Y. Cheng, *AIChE J., 34*(10), 1656 (1988).
6. A. A. Naujokas, *Plant/Oper. Prog., 4*(2), 120 (1985).
7. M. Petkovska, D. Tondeur, G. Grevillot, J. Granger, and M. Mitrović, *Sep. Sci. Technol., 26*(3), 425 (1991).
8. J. M. Klobucar and M. J. Pilat, *Environ. Prog., 11*(1), 11 (1992).
9. D. Basmadjian, *Can. J. Chem. Eng., 53*, 234 (1975).
10. D. Basmadjian, K. D. Ha, and C.-Y. Pan, *Ind. Eng. Chem., Process Des. Dev., 14*(3), 328 (1975).
11. R. Kumar and G. R. Dissinger, *Ibid., 25*, 456 (1986).
12. J. M. Schork and J. R. Fair, *Ind. Eng. Chem. Res., 27*(3), 457 (1988).
13. M. M. Davis and M. D. LeVan, *Ibid., 28*, 778 (1989).
14. S. Kulvaranon, M. E. Findley, and A. I. Liapis, *Ibid., 29*, 106 (1990).
15. K. J. Sladek, E. R. Gilliland, and R. F. Baddour, *Ind. Eng. Chem. Fundam., 13*(2), 100 (1974).
16. L. J. Petrovic and G. Thodos, *Ibid., 7*(2), 274 (1968).
17. D. M. Ruthven, *Principles of Adsorption and Adsorption Processes*, Wiley-Interscience, New York, 1984.
18. A. C. Hindmarsh, *ACM-SIGNUM Newslett., 15*(4), 10 (1980).
19. R. Forsythe, R. Madey, D. Rothstein, and M. Jaroniec, *Carbon, 26*(1), 98 (1989).
20. P. J. Photinos, A. Nordstrom, and R. Madey, *Ibid., 17*, 506 (1979).
21. R. Sips, *J. Chem. Phys., 16*, 490 (1948).
22. C.-C. Huang and J. R. Fair, *AIChE J., 35*(10), 1667 (1989).

Received by editor June 26, 1992
Revised March 18, 1993